

RESEARCH ARTICLE

The Influence of Smoothing Filtering Methods on the Performance of an EEG-Based Brain–Computer Interface

SALEH I. ALZHRANI¹ AND MASHAEL M. ALSALEH²¹Biomedical Engineering Department, College of Engineering, Imam Abdulrahman Bin Faisal University, Dammam 31441, Saudi Arabia²Information Technology Department, College of Computer and Information Sciences, King Saud University, Riyadh 11543, Saudi Arabia

Corresponding author: Saleh I. Alzahrani (sialzahrani@iau.edu.sa)

ABSTRACT Electroencephalography (EEG) recording is highly vulnerable to physiological or technical artifacts, which may reduce the performance of EEG-based brain–computer interface (BCI) systems. A number of noise artifact removal methods have been used to overcome this issue and hence estimate the cognitive state information much better, which will lead to the design of EEG-based BCI systems that are more practical, reliable, and accurate. Smoothing filter techniques are popularly used to remove noise and retain the morphology of signals. The purpose of this study is to compare three smoothing filters—median, Savitzky-Golay, and regularization—in the analysis of EEG data. To do so, we used publicly available motor imagery and P300 datasets to evaluate the effects of applying the aforementioned smoothing filters on the classification of right- versus left-hand imagery movements and target versus nontarget characters in spellers, respectively. The results show that smoothing EEG by regularization increased the coefficient of determination (r^2) values between the target and nontarget responses and slightly improved the signal-to-noise ratio relative to the other smoothing filters. Moreover, the results show that power spectral density for EEG smoothed by regularization reveals more discriminative information about left- and right-hand imagery movements. The classification results show that smoothing EEG by regularization provides the best classification accuracy in both datasets.

INDEX TERMS Electroencephalography, brain–computer interface, smoothing filters.

I. INTRODUCTION

Electroencephalography (EEG) is a technique developed by Hans Berger in 1929 for recording electrical activity in the brain [1]. Electrical signals formed by the action potentials of neurons in the brain are captured using EEG by placing small metal electrodes on the scalp. Compared with other technologies used to record brain activities, EEG reading technologies are relatively low cost and provide high-temporal-resolution data, in addition to being noninvasive. However, the nonlinearity and nonstationarity of the recorded signal and the low spatial resolution make the study of EEG signals challenging [2], [3]. Electroencephalogram (EEG) measurements of brain electrical activity reveal complicated

behavior with nonlinear dynamic features. This behavior manifests as EEG patterns of varying complexity [3]. Nonstationarity in EEG refers to changes in the statistical properties of the EEG signals over time, which can occur between intra- and inter-sessions. This can reduce the quality of the recorded signal, whereas most machine-learning algorithms are based on the assumption of data stationarity [4], [5].

The presence of noise in EEG recordings can cause nonstationarity in EEG signal. The term “noise” in EEG refers to any electrical activity that is recorded by the electrodes and is unrelated to the brain activity of interest. This electrical activity can arise from a variety of sources, including physiological noise, environmental interference, and electrical noise from recording equipment. Noise in EEG recordings can contribute to nonstationarity by obscuring or distorting the underlying brain signals, which can lead to changes in the

The associate editor coordinating the review of this manuscript and approving it for publication was Larbi Boubchir¹.

statistical properties of the EEG signal over time. Moreover, noise can introduce variability in the statistical features of the EEG signals, leading to fluctuations in the power and shape of the signal over time, thereby affecting the signal-to-noise ratio (SNR) and degrading the signal quality.

In addition to noise, several other factors can contribute to nonstationarity in EEG signals. Firstly, the physical features of EEG electrodes may deteriorate over time. For example, if the conductive gel dries up, the electrode impedance may change, or if the EEG cap is reused in a new session, the electrodes may shift position. Secondly, changes in neurophysiological factors, such as wakefulness. Thirdly, psychosocial factors, such as motivation, attention, and task engagement, cause significant differences. Fourthly, artifacts caused by body motions or muscle activity, such as swallowing or blinking, may change signal characteristics. Lastly, nonstationarity may occur as a result of neurofeedback; obtaining neurofeedback implies that users try to enhance outcomes by altering their brain patterns.

For the above reasons, EEG signals should be processed to maximize the SNR to reduce noise and improve signal quality to conduct a better analysis of the data. There are several preprocessing techniques that can be utilized to improve each type of EEG data. For example, S. Aydin has discussed several techniques to improve the auditory event-related potential type of EEG [6], [7].

One technique that can be used for all types of EEG data to improve signal quality is filtering. The filtering techniques can be classified into two types based on changes made to the signal: smoothing and nonsmoothing. Smoothing filters did not alter the signal waves' shapes as the nonsmoothing (classical) filters do [8]. Smoothing can be performed on individual trials. Consequently, a higher bit rate can be achieved as the user can make more selections in a shorter time [9].

In this work, filtering techniques based on smoothing the signal were used and compared in terms of improving the classification accuracy for two types of EEG signals: P300 and motor imagination-related event. Three mathematical models of different smoothing filters were developed and applied. These include median filter, Savitzky–Golay (SG), and regularization.

The median filter was selected as one of the filtering options in this study because of its simplicity of implementation, as well as its delicate signal smoothing and efficiency in filtering spikes. A median filter is a nonlinear filter that measures the average of sequences (in ascending order of data) around a processed point. The advantage of this filter is that it excludes values that deviate from the average [8], [10]. The median filter has been commonly applied in preprocessing EEG data, such as medical diagnosis in human, human emotion recognition, and motor imagery [8], [11], [12], [13].

The second applied smoothing filter is the SG filter. It is a least-square digital polynomial filter that smooths out irregularities and improves the SNR without altering the data appreciably. SG filtering, also called the least-square smoothing

filter method, is based on an existing mathematical procedure popularized by Savitzky and Golay in 1964, which publishes tables of convolution coefficients for various polynomials and subset sizes [14].

SG filter replaces each value of a signal series with a new value produced by applying polynomial fitting to a subset of contiguous data points. The fitting is done using linear least squares to $2n + 1$ nearby location, where n can be equal to or larger than the polynomial order. The more smoothly the signal develops, the more neighbors are employed in the averaging process. Smoothing with least squares reduces noise while preserving signal information [14], [15]. The SG filter has been utilized in smoothing and removing noise from event-related potentials in several studies. For example, SG was applied to smooth P300 [16] and to improve the analysis of error-related potential events [17], [18]. For motor imagination recognition, the SG filter has been applied as one of the steps to improve the recognition of motor imagination [19]. In addition, SG filter was employed to remove artifacts from EEG signals for neuromarketing applications [20].

The third smoothing technique applied in this study was regularization. Regularization, as used in mathematical terminology, is the process of adding a new term to an optimization problem to increase the “regularity” of the solution. In this study, the regularization presented by J. J. Stickel was applied [21]. In the context of EEG data, regularization was utilized to smooth P300 and compared with band-pass filter [9]. The objective of the study was to identify the occurrence of a target letter and not recognize it as a particular target letter. The study involved four participants (two impaired, and two unimpaired). The results showed that regularization outperforms bandpass filters in some cases, and vice versa [9].

Based on the literature survey that we performed, no previous study has compared regularization with other types of smoothing filters, as has been done in this paper. Given the nature of EEG data, filtering and smoothing the signal is an important step before starting to analyze the data. This paper provides a comparison of three types of smoothing filters and their effects on examining two types of EEG: P300 classification and motor imagery classification. This work contributes to, but not limited to, the field of BCI by demonstrating the use of smoothing by regularization method, which has been little used by researchers to analyze noisy data, to improve the performance of BCI system. The contribution of the present study will help the researchers who are working with noisy data to reduce noise and increase data quality more effectively. The rest of this paper is organized as follows. In Section II, we describe the two datasets used in this study. In Section III, we explain the smoothing filters applied. In Sections IV and VI, we list and discuss the results and main findings obtained from the experiments. Finally, we conclude this paper in Section VII.

II. DESCRIPTION OF DATASETS

A. P300 SPELLER PARADIGM DATASET

This dataset is publicly available on the brain–computer interface (BCI) competition webpage [22]. The Wadsworth Center, New York State Department of Health, initially provided it. The dataset was collected from one subject using the P300 speller developed by Farwell and Donchin in 1988 using BCI2000 software [23]. It was recorded from 64 electrodes arranged according to the standard 10–20 international electrode placement system. The recorded signals were bandpass filtered from 0.1 Hz to 60 Hz and sampled at 240 Hz. During the experiment, the subject was presented with a 6×6 matrix comprising 36 characters and asked to focus on characters in a word that was given by the investigator. Each row/column was intensified successively and randomly at a rate of 5.7 Hz. The intersection of the row and column with the desired (target) character elicited the P300 response. The dataset consisted of three sessions. In each session, a total of 15 runs were performed for each character. For each run, each row/column was flashed randomly for 100 ms, followed by a blank period of 75 ms. The dataset was split into training and testing datasets. The training dataset had 1,260 signal samples for the P300 responses and 6,300 signal samples for the non-P300 responses. The testing dataset had 930 signal samples for the P300 responses and 4,650 signal samples for the non-P300 responses.

B. MOTOR IMAGERY DATASET

This dataset was provided by the Berlin BCI group [24]. It consists of EEG recorded from nine healthy subjects. The data were collected from three electrodes (C3, Cz, and C4), filtered between 0.5 Hz and 100 Hz, and sampled at 250 Hz. The subjects' tasks were to imagine right/left-hand movements without feedback based on a visual cue (an arrow) presented on a computer screen for 1.25 s. The subjects were asked to imagine left- and right-hand movements for a period of 4 s. Each subject participated in 12 runs, with 10 trials each. This resulted in 120 trials of each hand movement.

III. SMOOTHING METHODS

In this paper, three different smoothing methods were applied to the EEG datasets. The median filter is a well-known order-statistic filtering technique used for noise suppression. It was first introduced by J. W. Tukey in 1974 [25]. In the median filter, each sample in the signal is replaced with the median of the samples contained in a window around that sample, as follows:

$$\mathbf{Y}(\mathbf{n}) = \text{med}[\mathbf{X}(\mathbf{n} - \mathbf{k}), \dots, \mathbf{X}(\mathbf{n}), \dots, \mathbf{X}(\mathbf{n} + \mathbf{k})] \quad (1)$$

where $\mathbf{X}(\mathbf{n})$ and $\mathbf{Y}(\mathbf{n})$ are the n th samples of input and output sequences, respectively, the window size is $\mathbf{N} = 2\mathbf{k} + 1$, and med is the median function.

SG filtering is a simple and smoothing technique with a low computational cost originally proposed by Savitzky and Golay in 1964 [14]. The SG smoothing filter is typically used in digital signal processing to smooth a noisy signal

based on the local least-squares polynomial approximation method [18]. In SG filtering, a polynomial fitting method is applied to successive subsets of adjacent data samples in a prescribed window. The window size and the polynomial degree are two parameters that can be used to control smoothing [20].

If the data consist of a set of points $\{\mathbf{x}_j, \mathbf{y}_j\}$, $\mathbf{j} = 1, 2, \dots, \mathbf{n}$, where \mathbf{x}_j is an independent variable and \mathbf{y}_j is an actual value, a set of m convolution coefficients, \mathbf{C}_i , the smoothed data \mathbf{Y}_j can be calculated as follows:

$$\mathbf{Y}_j = \sum_{i=\frac{1-m}{2}}^{\frac{m-1}{2}} \mathbf{C}_i \mathbf{y}_{j+i}, \quad \text{where } \frac{m-1}{2} < \mathbf{j} < \mathbf{n} - \frac{m-1}{2} \quad (2)$$

The third method used in this work was introduced by J. Stickel in 2010 [21]. Smoothing by regularization is simple and easy to implement compared with other smoothing techniques. In this method, the data are smoothed by regularization, in which a quadratic term is used for regularization. In (3), $\mathbf{y}(\mathbf{x})$ is a set of data, where $\mathbf{i} = 1, 2, \dots, \mathbf{N}$; $\hat{\mathbf{y}}(\mathbf{x})$ is a smooth function that approximates $\mathbf{y}(\mathbf{x})$; and λ is the regularization parameter.

$$\mathbf{Q}(\hat{\mathbf{y}}) = \int_{\mathbf{x}1}^{\mathbf{xN}} |\hat{\mathbf{y}}(\mathbf{x}) - \mathbf{y}(\mathbf{x})|^2 \mathbf{d}\mathbf{x} + \lambda \int_{\mathbf{x}1}^{\mathbf{xN}} |\hat{\mathbf{y}}^{(d)}(\mathbf{x})|^2 \mathbf{d}\mathbf{x} \quad (3)$$

Equation (3) has two terms: the squared error and the roughness term of $\hat{\mathbf{y}}(\mathbf{x})$ multiplied by λ . Both terms have to be minimized to get a good fit and approximation of $\mathbf{y}(\mathbf{x})$. It is recommended to choose a small value for λ , as it minimizes the squared error. To choose an appropriate value λ , the generalized cross-validation (GCV) and the classification accuracy were computed for steps of λ ranges between 1×10^{-5} and 0.1. The value of 0.001 resulted in the minimum GCV and the best classification accuracy.

IV. METHODOLOGY

A. DATA PREPROCESSING AND FEATURE EXTRACTION

Both datasets were preprocessed before the feature extraction and classification steps. For the P300 dataset, the data samples were extracted for each channel from -200 ms to 660 ms around the presentation of each stimulus, where the pre-stimulus interval was used for baseline correction and SNR calculation. The post-stimulus time window (0 ms to 660 ms) was extracted as a temporal feature since this time window is enough to capture all necessary information required for an efficient classification, as the P300 signal appears approximately 300 ms after the stimulus. Next, each EEG segment was filtered using 8th-order bandpass Chebyshev filter of Type I with cut-off frequency lying between 0.1 and 20 Hz. The means of all post-stimulus signals from each channel were then concatenated into a single feature vector. This was used as the input to the classifier.

For the motor imagery (MI) dataset, spectral power synchronization and desynchronization in the mu (μ) frequency band were extracted. To extract relevant features, the power

spectral density (PSD) for each EEG trial on each channel was estimated using Welch’s method. The EEG data were split into a short-time Hanning window T centered at peaks τ_q , where $q = 1, 2$ is the time window at different hand movement. Then, for each window, the discrete Fourier transform (DFT) was computed. Finally, all the DFTs were scaled and averaged together as follows:

$$P_n(f, \tau_q) = \frac{1}{T} \left| \sum_{t=-\frac{T}{2}}^{\frac{T}{2}-1} X_n(\tau_q+t) |H(t)| \exp(i\frac{2\pi}{T}(f-1)t) \right|^2 \quad (4)$$

where $P_n(f, \tau_q)$ is the PSD at frequency f and time τ_q on channel n , $H(t)$ is the Hanning window, and T is the window length. Next, the PSDs for each trial were normalized as follows.

$$\tilde{P}_n(f, m) = \ln(P_n(f, m)) - \ln\left(\frac{1}{M} \sum_{p=1}^M P_n(f, m)\right) \quad (5)$$

where the normalized PSD $p_n(f, m)$ is the log-transferred division between the PSD of each segment data and the mean of all segment data. The symbols f, m, n , and M denote frequency, segment, channel numbers, and the total number of segments, respectively. Finally, the spectral powers changes at μ band (8–12 Hz) were chosen as movement-related features to decode different hand movements.

B. SNR AND r^2 VALUES CALCULATIONS

To compare the smoothing techniques used in this study, two parameters were calculated for the P300 dataset. The first parameter, SNR, was calculated at each electrode by dividing the P300 peak amplitude by the peak across the baseline variance (-200 ms to 0 ms) [29]. The P300 peak amplitude was determined by the maximum positive amplitude in the time window between 300 ms and 350 ms. Mathematically, the SNR is commonly defined as shown in (6).

$$SNR = \frac{\bar{y}_{tw}}{\sigma_M} \quad (6)$$

where \bar{y}_{tw} is the average event-related potential (ERP) amplitude computed within the time window between 300 ms and 350 ms, and σ_M is the baseline variance.

The second parameter that was computed to compare the smoothing techniques is the coefficient of determination (r^2 , the squared value of Pearson’s r). The r^2 is used to measure the separability between two classes (e.g., target and nontarget classes). It can be computed using (7).

$$r^2(x, y) = \frac{N_1 N_2}{(N_1 + N_2)^2} \frac{(\mu_1 - \mu_2)^2}{\text{var}(x_i)} \quad (7)$$

where $\mu_1 = \text{mean}(x_i)_{y_i=1}$ and $\mu_2 = \text{mean}(x_i)_{y_i=2}$ are the class means and $N_k = |\{i | y_i = k\}|$ is the number of samples of class k .

C. CLASSIFICATION PROCEDURES

This research employed linear discriminant analysis (LDA), a well-known classification method in machine learning and pattern recognition, to classify target versus nontarget and right versus left-hand imagery movements, respectively. The LDA is a supervised learning method that is used to find a linear combination of features that separate two or more classes of objects.

Based on the features extracted from each EEG segment, The data was randomly partitioned into two subsets, with 80% of the data used for training and 20% of the data used for testing. The LDA classifier was trained on the 80% of the data using 5-fold cross-validation. During each fold of the cross-validation process, the data was randomly split into five equal-sized parts with four parts used for training and one part used for validation. This process was repeated five times, with each part used for validation once. The performance of the LDA classifier is evaluated on the remaining 20% of the data.

V. RESULTS

Two datasets were used in this study to investigate the effects of different smoothing methods on ERPs. The first dataset consisted of ERPs recorded from one subject using 64 electrodes during the P300 speller experiment. The second dataset was collected from the C3, C4, and Cz electrodes, while nine subjects performed imagery left/right-hand movement. For both datasets, classification was performed using a linear discriminant analysis (LDA) classifier.

Fig.1(a) shows the grand averages of the ERP waveforms of P300 (in blue) and non-P300 (in black) at the Cz electrode during the experiment. Clearly, the subject responded strongly to the visual stimulus, where he produced a higher amplitude of the target signal compared to the nontarget signal. Fig.1(a) also shows the r^2 values between the P300 and non-P300 conditions averaged from one subject on site Cz. The maximal window for the P300 response is approximately 300–350 ms. Fig.1(b) illustrates the topographic maps of the distribution of voltage at different latency windows for target and nontarget conditions. The latency window between 290 ms and 380 ms for the target condition clearly shows greater central P300 amplitude relative to the nontarget condition.

Fig.2 shows the averaged PSD of the imagery left-and right-hand movements from one subject recorded from the C3 and C4 electrodes. The PSD was calculated for each channel using Welch’s method [30]. In this study, movement-related spectral changes were used as features to classify left- and right-hand imagery movements. In Fig.2, we can clearly see that hand movement elicits power decreases (event-related desynchronization) in the μ band (8–12 Hz) over the contralateral cortex.

Fig.3 illustrates the effect of using different smoothing methods on the P300 signals. We can see that applying smoothing methods slightly affects the overall shape of the signal. In addition, smoothing the signal by regularization

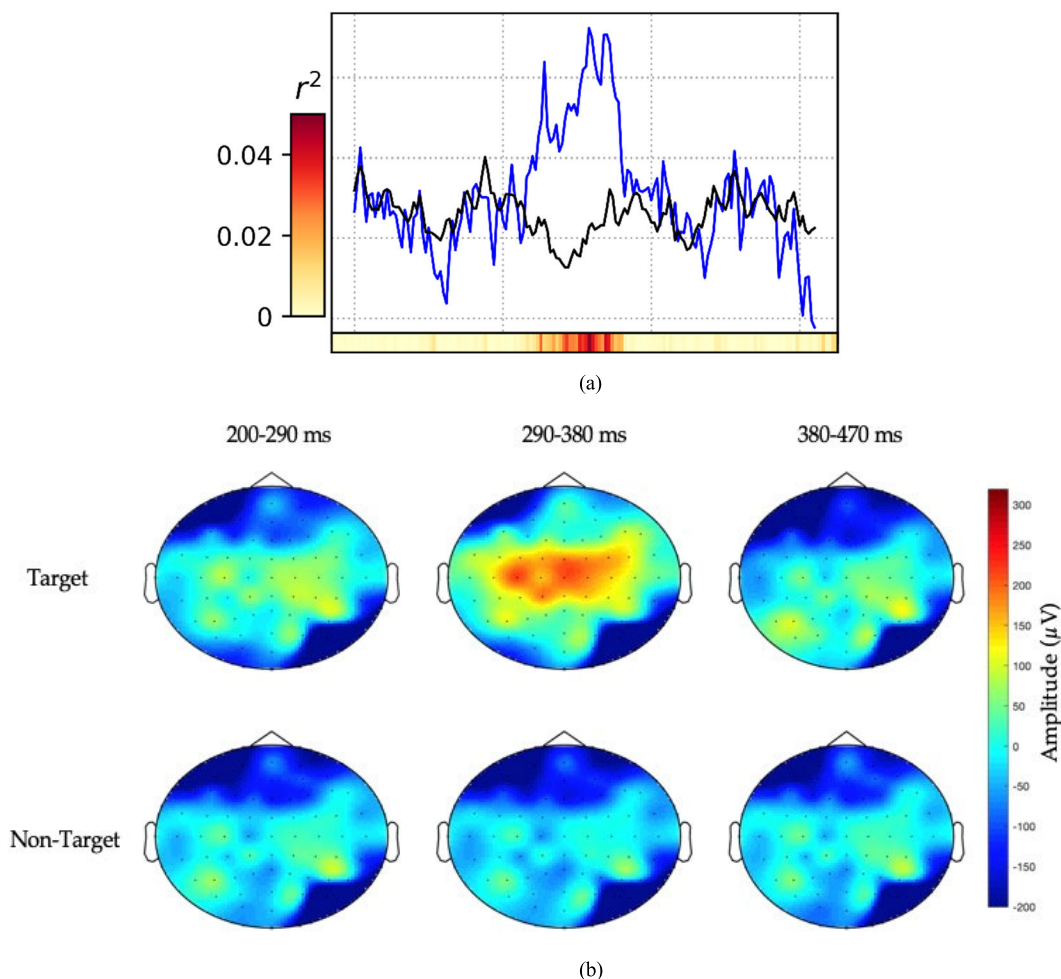


FIGURE 1. (a) Grand average of P300 amplitudes recorded at channel Cz. Target response is presented in blue, and nontarget response is presented in black with color coded r^2 -values for the difference between target and nontarget responses. X-axis, latency (ms); Y-axis, amplitude (μV) (b) P300 topography maps for target and nontarget conditions for different latency windows. The color bar shows the amplitude in μV .

tends to provide better results in terms of removing noise. This result suggests that smoothing the signal by regularization can better reduce the impact of noise and enhance the signal of interest, leading to an increase in the SNR. This increase in the SNR can improve the quality of the signal and make it easier to distinguish signal components from noise components. As a result, classification algorithms can be more accurate and robust, leading to better classification performance.

Fig.4 (a) shows the averaged r^2 values between the P300 and non-P300 signals filtered by the bandpass filter and smoothed by the SG filter, regularization, and median filter. As shown in Fig.4 (a), the differences in ERPs between target and nontarget stimuli were larger when the signals were smoothed by regularization ($r^2 = 0.008 \pm 0.004$) compared to those observed when the signals were bandpass filtered ($r^2 = 0.0061 \pm 0.003$), smoothed by the SG filter ($r^2 = 0.0072 \pm 0.003$), and smoothed by the median filter

($r^2 = 0.007 \pm 0.003$), with no significant difference between them ($p > 0.05$). Fig.4 (b) shows the topographic maps of r^2 -values during the presentation of target stimuli after applying different smoothing techniques. It can be seen that higher P300 responses elicited by the target stimuli were more prominent when smoothing data by regularization, as higher r^2 -values were obtained compared to other smoothing techniques.

In this study, we investigated the effect of different smoothing filtering methods on the SNRs of ERP signals. The SNRs for the P300 signals were calculated by dividing the maximum voltage amplitude in the time window between 300 and 400 ms by the peak across the baseline variance (-200 ms to 0 ms). Fig.5 compares the SNRs of the P300 signals smoothed by the different smoothing filters. The mean SNRs were 0.95 ± 0.24 , 1.07 ± 0.22 , 1.13 ± 0.22 , and 0.98 ± 0.20 when the signals were filtered by bandpass, SG, regularization, and median smoothing filters, respectively. Smoothing

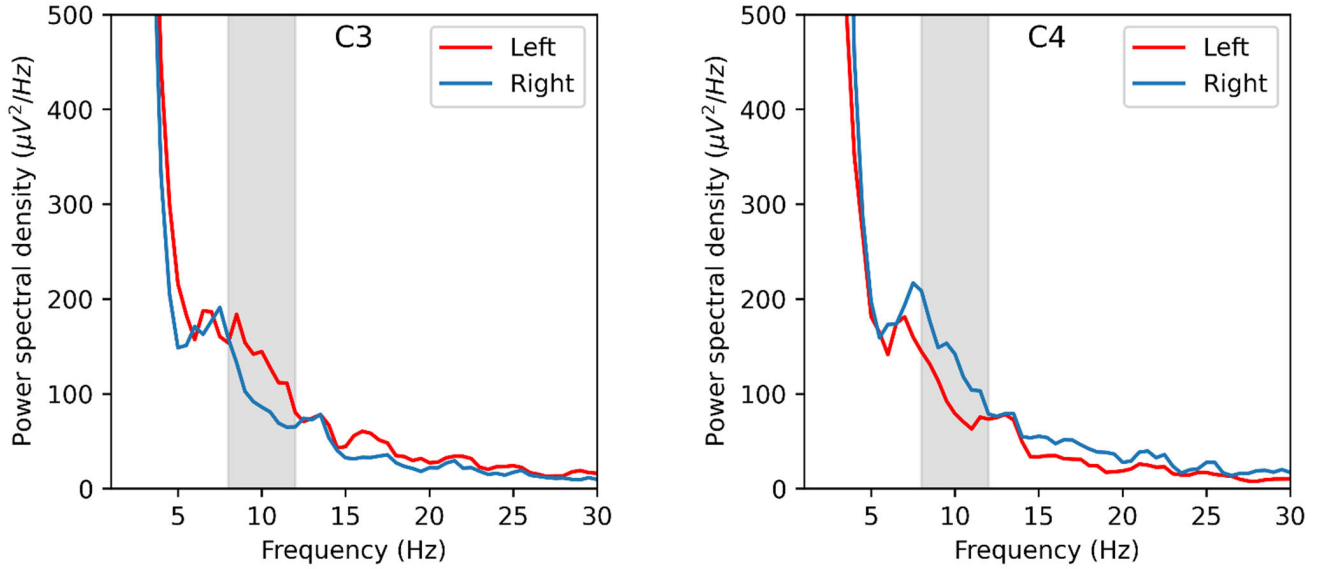


FIGURE 2. The PSD of the left- (red) and right (blue)-hand imagery movements from C3 and C4 electrodes.

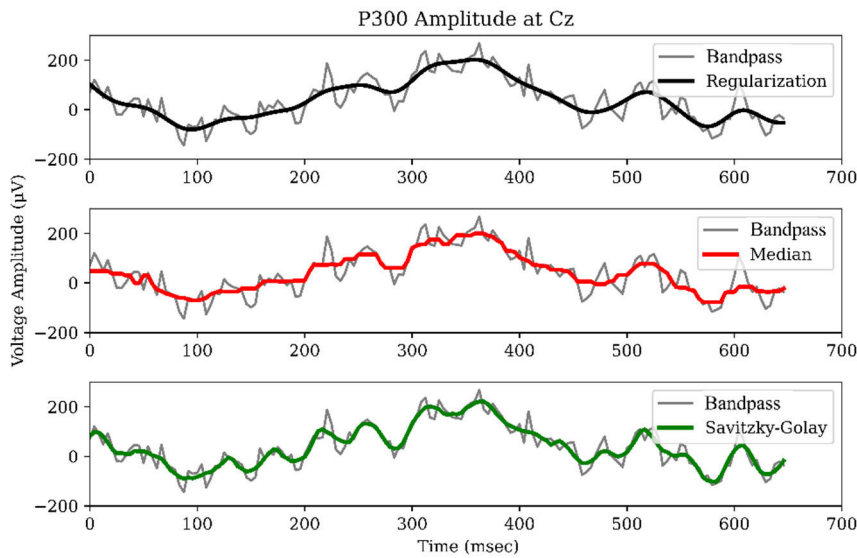


FIGURE 3. P300 signals smoothed by bandpass filter, regularization, median filter, and Savitzky-Golay filter.

the signals by regularization increased the SNR relative to other smoothing filter techniques. However, the difference in SNR values was not significant.

Fig.6 shows the averaged PSDs of EEG over the left (C3 electrode) and right (C4 electrode) motor cortex corresponding to imaginations of left and right-hand movements after the implementation of different smoothing techniques on the EEG signals. The PSD was estimated for the μ band for each electrode. Left- and right-hand imagery movements induced an increase and decrease in the μ band at both electrodes. As shown in Fig.6, compared to other smoothing techniques, smoothing the EEG by regularization enhanced the mean

power difference between left- and right-hand imagery movements. This finding suggests that smoothing EEG by regularization will increase the classification accuracy of the discrimination between the left- and right- hand movements.

Using temporal EEG data for the P300 dataset and ERS/ERD from μ frequency band for the motor imagery dataset as features, each dataset was classified using the LDA classifier to target versus nontarget and right versus left-hand imagery movements, respectively. The classification results are shown in Table 1. For the P300 dataset, the best classification accuracy was obtained when the data were smoothed by regularization, showing a classification accuracy of 94.05%.

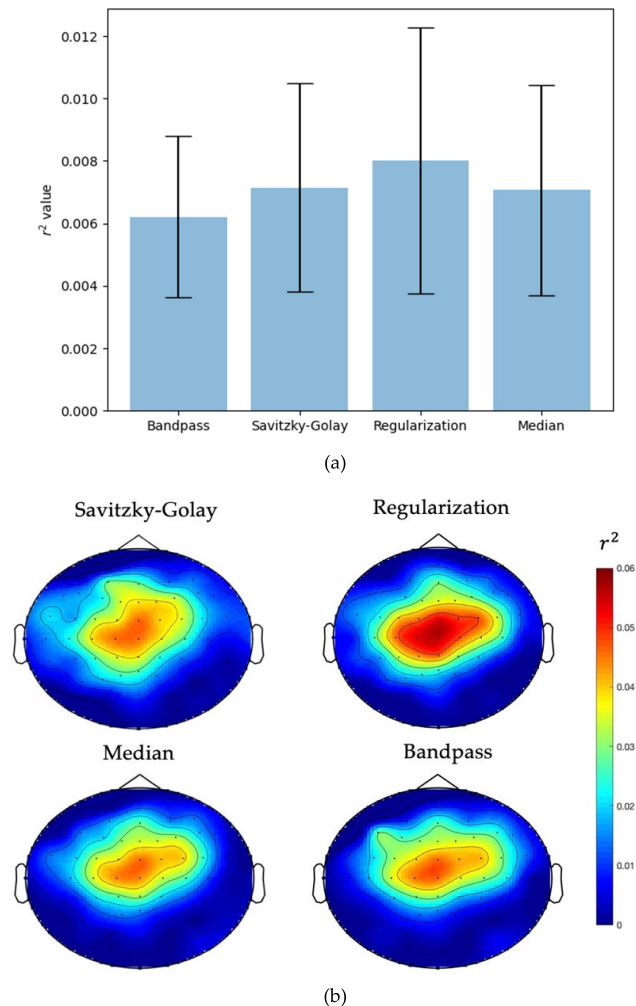


FIGURE 4. (a) Comparison of r^2 -values obtained for the P300 signal filtered by bandpass filter and smoothed by the Savitzky-Golay filter, regularization, and median filter (b) comparison of the topographic maps of r^2 -values after applying different smoothing techniques.

Smoothing the data by median and SG filters yielded higher classification accuracy than when the data were filtered by bandpass filter, showing classification accuracies of 88.94%, 90.11%, and 84.2%. These results were consistent with the r^2 results in Fig.4.

The results of the binary class classification of the imagery EEG patterns corresponding to the right- and left-hand imagery movements are presented in Table 1. The average classification accuracies were $90.12\% \pm 1.05\%$, $88.78\% \pm 2.02\%$, and $84.31\% \pm 2.32\%$ when the data were smoothed by regularization, SG, and median filters, respectively. The lower classification accuracy obtained was $82.22\% \pm 1.45\%$, where the data were filtered by bandpass filter. The superior classification results suggest that smoothing ERPs by regularization contributes to enhancing BCI classification and hence improves the communication and control capabilities of those suffering from severe neuromuscular disorders.

VI. DISCUSSION

In the last several decades, there has been growing interest in developing new methods to design more robust and reliable EEG-based BCI systems to reestablish communication and control for severely disabled people. However, the use of EEG as an input to the system has limited the potential to design practical and useful BCI systems because of its low spatial resolution and SNRs. A number of denoising techniques have been developed for preventing noise in EEG and hence increasing SNRs [31], [32], [33]. Some of these techniques include signal averaging, filtering, principal component analysis, independent component analysis, and parallel factor analysis [36]. The study presented in this paper has investigated the effect of three different smoothing filters in removing noise from EEG signals and in classifying two different types of ERPs: P300 for classifying target versus nontarget and MI for classifying left- versus right-hand movement imagination.

EEG recording is highly vulnerable to various forms of sources of noise such as muscle movements, eye blinks, power source, which are unavoidable. Denoising step is a crucial step in the preprocessing stage of the EEG signal to obtain useful information that reflects certain cognitive state and to facilitate the process of feature extraction. For the P300 based-BCI system, the well-known feature of interests is narrow band cognitive response around 300 ms after the stimulus. As it is shown in Fig.3, the signals become less noisy when they are smoothed by different smoothing methods. In comparison to other smoothing methods used in this study, smoothing the signals by regularization is the most effective method for removing unwanted high-frequency components.

For classifying P300, our results show that smoothing the signal captured from Cz improves the signal shape in general, where regularization was the best filter in terms of removing noise, as clearly shown in Fig.3. This was also supported by the r^2 value (coefficient of determination), which quantifies the overall signal variance that the task condition determines (target vs. nontarget) [35]. Smoothing signals by regularization show the highest values of r^2 , which was also reflected in the classification accuracies (Table 1), with the highest classification accuracy of 94.05% compared to the other smoothing filters. Compared with the literature [9], the current study shows that regularization outperforms bandpass filters in some cases. However, P300 was captured in different task types, and some subjects were impaired, which made comparison difficult. To classify motor imagination, that is, (right vs. left) hand imagery movement imagination, we used PSD for feature extraction and LDA as the classifier. The results in Table 1 illustrate that regularization improved the classification accuracy by 1.34% in comparison to the SG filter.

The filtering techniques applied in this study can be divided into two groups, based on how the signal is smoothed. The first group includes smoothing filters that rely on smoothing

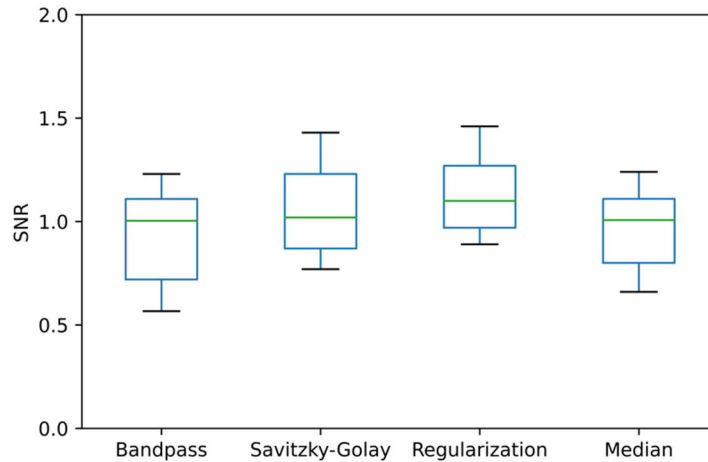


FIGURE 5. (a) The PSD box-plot comparing the SNR of different smoothing filter techniques ($p > 0.05$).

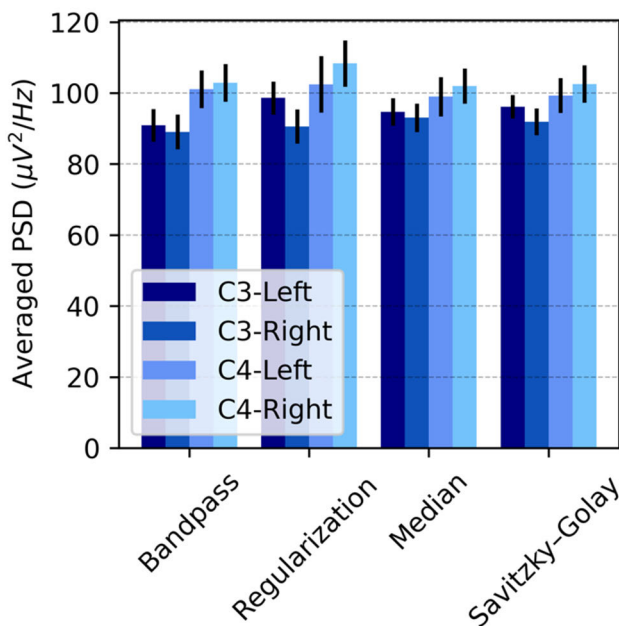


FIGURE 6. The averaged PSD values at C3 and C4 electrodes across all subjects for left- and right-hand imagery movements for different smoothing techniques.

the signal without distorting the wave shape or removing any values. This group includes SG and regularization.

In comparison, the other group of smoothing filters allows the signal to be processed. For example, a bandpass allows only the signal between two specific bands to pass. In median filters, all the values that differ from the average of the signal are excluded. Our results show that SG and regularization outperform bandpass and median filters. Regularization provides the best results in terms of SNR and classification accuracy in the two datasets. This kind of comparison between the two types of filters has been conducted in the literature. For example, a smoothing filter based on SG were proposed and compared with some other EEG data filtering approaches. The SG-based filter outperformed the other filters in terms of average peak coverage [36].

To the best of our knowledge, this is the first study to apply regularization in smoothing motor imaginary EEG data, and we can conclude that it provides results relatively close to SG's. This study has some limitations that will be addressed in future work. For example, the proposed methodology was applied to two types of EEG data: P300 and motor imagination. It should be examined on other types of EEG, such as auditory event-related potentials. In addition, different feature extraction techniques can be applied with each smoothing filter. Also, EEG data collected by different EEG devices have different qualities, which can affect the type

TABLE 1. Classification accuracies of four filtering methods for P300 and MI datasets.

Filtering Method	Accuracy (%)	
	P300 dataset	MI dataset
Bandpass	84.2	82.22 ± 1.45
Savitzky-Golay	90.11	88.78 ± 2.02
Regularization	94.05	90.12 ± 1.05
Median	88.94	84.31 ± 2.32

of smoothing technique required. Moreover, the parameters of smoothing filtering methods applied in this study were fixed (for both regularization and Savitzky–Golay), while the influence of those filters varies based on the selected parameters [8], [9].

VII. CONCLUSION

The EEG-based BCI system performance has long been limited by its ability to extract meaningful information from recorded signals due to external and internal noise and artifacts. The development of brain–computer interfaces may be advanced, and many solutions involving the use of EEG data may be improved with the proper choice of filtering. Where most of these BCI applications are dedicated to help individual with physical disabilities. For example, controlling spellers, directing wheelchairs, post-stroke motor rehabilitation, controlling artificial body parts, and controlling sensors in smart houses [37].

In this study, we examined different smoothing filters to remove noise from EEG signals. Our results suggest that smoothing EEG using the regularization method improves the classification accuracy of ERPs more than median and SG filters do. Future work will involve further testing different EEG data to determine whether there is consistent performance. In addition, we will apply optimization methods to choose an appropriate value for the regularization parameter. We will also compare smoothing data by regularization with state-of-the-art artifact removal techniques.

REFERENCES

- [1] H. Berger, “Über das elektroencephalogramm des menschen,” *Archiv für Psychiatrie und Nervenkrankheiten*, vol. 87, no. 1, pp. 527–570, 1929.
- [2] B.-K. Min, M. J. Marzelli, and S.-S. Yoo, “Neuroimaging-based approaches in the brain–computer interface,” *Trends Biotechnol.*, vol. 28, no. 11, pp. 552–560, Nov. 2010, doi: [10.1016/j.tibtech.2010.08.002](https://doi.org/10.1016/j.tibtech.2010.08.002).
- [3] K. Natarajan, R. Acharya U, F. Alias, T. Tiboleng, and S. K. Puthusserypady, “Nonlinear analysis of EEG signals at different mental states,” *Biomed. Eng. OnLine*, vol. 3, no. 1, pp. 1–11, Dec. 2004.
- [4] P. Shenoy, M. Krauledat, B. Blankertz, R. P. N. Rao, and K.-R. Müller, “Towards adaptive classification for BCI,” *J. Neural Eng.*, vol. 3, no. 1, p. R13, Mar. 2006.
- [5] Z. Khademi, F. Ebrahimi, and H. M. Kordy, “A review of critical challenges in MI-BCI: From conventional to deep learning methods,” *J. Neurosci. Methods*, vol. 383, Jan. 2023, Art. no. 109736.
- [6] S. Aydın, “Tikhonov regularized solutions for improvement of signal-to-noise ratio in case of auditory-evoked potentials,” *Med. Biol. Eng. Comput.*, vol. 46, no. 10, pp. 1051–1056, Oct. 2008.
- [7] S. Aydın, “A new combination: Scale-space filtering of projected brain activities,” *Med. Biol. Eng. Comput.*, vol. 47, no. 4, pp. 435–440, Apr. 2009.
- [8] A. Kawala-Sterniuk, M. Podpora, M. Pelc, M. Blaszczyzyn, E. J. Gorzelanczyk, R. Martinek, and S. Ozana, “Comparison of smoothing filters in analysis of EEG data for the medical diagnostics purposes,” *Sensors*, vol. 20, no. 3, p. 807, Feb. 2020, doi: [10.3390/s20030807](https://doi.org/10.3390/s20030807).
- [9] R. Ashari and C. Anderson, “EEG subspace analysis and classification using principal angles for brain–computer interfaces,” in *Proc. IEEE Symp. Comput. Intell. Brain Comput. Interfaces (CIBCI)*, Dec. 2014, pp. 57–63, doi: [10.1109/CIBCI.2014.7007793](https://doi.org/10.1109/CIBCI.2014.7007793).
- [10] P. Puzdrowska, “Signal filtering method of the fast-varying diesel exhaust gas temperature,” *Combustion Engines*, vol. 175, no. 4, pp. 48–52, 2018.
- [11] N. Thammasan, K. Fukui, and M. Numao, “An investigation of annotation smoothing for EEG-based continuous music-emotion recognition,” in *Proc. IEEE Int. Conf. Syst., Man, Cybern. (SMC)*, Oct. 2016, pp. 003323–003328.
- [12] M. Li, R. Wang, J. Yang, and L. Duan, “An improved refined composite multivariate multiscale fuzzy entropy method for MI-EEG feature extraction,” *Comput. Intell. Neurosci.*, vol. 2019, pp. 1–12, Mar. 2019.
- [13] K. S. Bhanumathi, D. Jayadevappa, and S. Tunga, “Feedback artificial shuffled shepherd optimization-based deep maxout network for human emotion recognition using EEG signals,” *Int. J. Telemedicine Appl.*, vol. 2022, pp. 1–14, Jan. 2022.
- [14] A. Savitzky and M. J. E. Golay, “Smoothing and differentiation of data by simplified least squares procedures,” *Anal. Chem.*, vol. 36, no. 8, pp. 1627–1639, Jul. 1964.
- [15] S. Jahani, S. K. Setarehdan, D. A. Boas, and M. A. Yücel, “Motion artifact detection and correction in functional near-infrared spectroscopy: A new hybrid method based on spline interpolation method and Savitzky–Golay filtering,” *Neurophotonics*, vol. 5, no. 1, 2018, Art. no. 015003.
- [16] S. C. Chen, A. R. See, C. K. Liang, and Y. Y. Lee, “Evaluating the performance of the P300-based brain computer interface for the LEGO page turner,” in *Proc. 2nd Int. Conf. Intell. Technol. Eng. Syst. (ICITES)*, 2014, pp. 765–771.
- [17] S. Bhattacharyya, A. Konar, D. N. Tibarewala, and M. Hayashibe, “A generic transferable EEG decoder for online detection of error potential in target selection,” *Frontiers Neurosci.*, vol. 11, p. 226, May 2017, doi: [10.3389/fnins.2017.00226](https://doi.org/10.3389/fnins.2017.00226).
- [18] T. Li and Z. Huang, “An approach to detecting ErrP elicited by feedback of P300 speller BCI based on coefficients of determination,” in *Proc. 13th Int. Congr. Image Signal Process., Biomed. Eng. Informat. (CISP-BMEI)*, Oct. 2020, pp. 506–510, doi: [10.1109/CISP-BMEI51763.2020.9263583](https://doi.org/10.1109/CISP-BMEI51763.2020.9263583).
- [19] M. Shorif, U. Jagdish, and C. Bansal, “EEG motor signal analysis-based enhanced motor activity recognition using optimal de-noising algorithm,” in *Proc. Int. Joint Conf. Comput. Intell.*, 2019, pp. 125–136. [Online]. Available: <http://www.springer.com/series/16171>
- [20] S. M. A. Shah, S. M. Usman, S. Khalid, I. U. Rehman, A. Anwar, S. Hussain, S. S. Ullah, H. Elmannai, A. D. Algarni, and W. Manzoor, “An ensemble model for consumer emotion prediction using EEG signals for neuromarketing applications,” *Sensors*, vol. 22, no. 24, p. 9744, Dec. 2022.
- [21] J. J. Stickel, “Data smoothing and numerical differentiation by a regularization method,” *Comput. Chem. Eng.*, vol. 34, no. 4, pp. 467–475, Apr. 2010, doi: [10.1016/j.compchemeng.2009.10.007](https://doi.org/10.1016/j.compchemeng.2009.10.007).
- [22] B. Blankertz. *BCI Competition II*. [Online]. Available: <http://ida.first.fhg.de/projects/bci/competition/>
- [23] G. Schalk, D. J. McFarland, T. Hinterberger, N. Birbaumer, and J. R. Wolpaw, “BCI2000: A general-purpose brain–computer interface (BCI) system,” *IEEE Trans. Biomed. Eng.*, vol. 51, no. 6, pp. 1034–1043, Jun. 2004.
- [24] B. Blankertz, G. Dornhege, M. Krauledat, K.-R. Müller, and G. Curio, “The non-invasive Berlin brain–computer interface: Fast acquisition of effective performance in untrained subjects,” *NeuroImage*, vol. 37, no. 2, pp. 539–550, Aug. 2007.
- [25] J. W. Tukey, “Nonlinear (nonsuperposable) methods for smoothing data,” *Proc. Cong. Rec. EASCOM*, vol. 74, pp. 673–681, 1974.
- [26] G. Vivó-Truyols and P. J. Schoenmakers, “Automatic selection of optimal Savitzky–Golay smoothing,” *Anal. Chem.*, vol. 78, no. 13, pp. 4598–4608, 2006.
- [27] P. H. C. Eilers, “A perfect smoother,” *Anal. Chem.*, vol. 75, no. 14, pp. 3631–3636, Jul. 2003.
- [28] A. S. Lubansky, Y. L. Yeow, Y.-K. Leong, S. R. Wickramasinghe, and B. Han, “A general method of computing the derivative of experimental data,” *AICHE J.*, vol. 52, no. 1, pp. 323–332, Jan. 2006.
- [29] N. N. Thigpen, E. S. Kappenman, and A. Keil, “Assessing the internal consistency of the event-related potential: An example analysis,” *Psychophysiology*, vol. 54, no. 1, pp. 123–138, Jan. 2017.
- [30] O. M. Solomon Jr., “PSD computations using Welch’s method. [power spectral density (PSD)],” Sandia Nat. Labs., Albuquerque, NM, USA, Tech. Rep. 92, 1991.
- [31] Z. A. A. Alyasseri, A. T. Khader, M. A. Al-Betar, X.-S. Yang, M. A. Mohammed, K. H. Abdulkareem, S. Kadry, and I. Razzak, “Multi-objective flower pollination algorithm: A new technique for EEG signal denoising,” *Neural Comput. Appl.*, vol. 35, pp. 1–20, Jan. 2022.

- [32] E. Brophy, P. Redmond, A. Fleury, M. De Vos, G. Boylan, and T. Ward, "Denoising EEG signals for real-world BCI applications using GANs," *Frontiers Neuroergonomics*, vol. 2, p. 44, Jan. 2022.
- [33] H. Zhang, C. Wei, M. Zhao, Q. Liu, and H. Wu, "A novel convolutional neural network model to remove muscle artifacts from EEG," in *Proc. IEEE Int. Conf. Acoust., Speech Signal Process. (ICASSP)*, Jun. 2021, pp. 1265–1269.
- [34] M. M. N. Mannan, M. A. Kamran, and M. Y. Jeong, "Identification and removal of physiological artifacts from electroencephalogram signals: A review," *IEEE Access*, vol. 6, pp. 30630–30652, 2018.
- [35] *Glossary—BCI2000 Wiki*. Accessed: Mar. 5, 2023. [Online]. Available: <https://www.bci2000.org> and <https://www.bci2000.org/mediawiki/index.php/Glossary>
- [36] N. Browarska, A. Kawala-Sterniuk, J. Zygarlicki, M. Podpora, M. Pelc, R. Martinek, and E. Gorzelańczyk, "Comparison of smoothing filters' influence on quality of data recorded with the emotiv EPOC flex brain-computer interface headset during audio stimulation," *Brain Sci.*, vol. 11, no. 1, p. 98, Jan. 2021.
- [37] M. Soufneyestani, D. Dowling, and A. Khan, "Electroencephalography (EEG) technology applications and available devices," *Appl. Sci.*, vol. 10, no. 21, p. 7453, Oct. 2020.

techniques for analyzing electroencephalography (EEG) signals in noninvasive brain-computer interfaces (BCIs) and statistical signal processing and its application in the field of biomedical engineering.

MASHAEL M. ALSALEH received the Ph.D. degree in computer sciences from The University of Sheffield, U.K., in 2019. She is currently an Assistant Professor with the Information Technology Department, College of Computer and Information Sciences, King Saud University, Riyadh, Saudi Arabia. Her research interests include brain-computer interface (algorithms, systems, adaptation, and applications), machine learning and pattern recognition, artificial intelligence, and human-computer interface (assistive technologies and interaction design).

• • •



SALEH I. ALZHRANI received the B.S. degree in electrical engineering from Umm Al-Qura University, Saudi Arabia, in 2014, and the M.S. and Ph.D. degrees in biomedical engineering from Colorado State University, Fort Collins, CO, USA, in 2016 and 2019, respectively. He is currently an Assistant Professor with the Biomedical Engineering Department, Imam Abdulrahman Bin Faisal University, Dammam, Saudi Arabia. His research interests include developing machine learning